Scaling of Entanglement Entropy at Deconfined Quantum Criticality

Jiarui Zhao,[1] Yan-Cheng Wang,[2] Zheng Yan,[1,3] Meng Cheng,[4,*] and Zi Yang Meng[1,†]
[1]Department of Physics and HKU-UCAS Joint Institute of Theoretical and Computational Physics, The University of Hong Kong, Pokfulam Road, Hong Kong SAR, China
[2]School of Materials Science and Physics, China University of Mining and Technology, Xuzhou 221116, China
[3]State Key Laboratory of Surface Physics and Department of Physics, Fudan University, Shanghai 200438, China
[4]Department of Physics, Yale University, New Haven, Connecticut 06520-8120, USA

(Received 19 July 2021; accepted 24 November 2021; published 3 January 2022)

We develop a nonequilibrium increment method to compute the Rényi entanglement entropy and investigate its scaling behavior at the deconfined critical (DQC) point via large-scale quantum Monte Carlo simulations. To benchmark the method, we first show that, at a conformally invariant critical point of O(3) transition, the entanglement entropy exhibits universal scaling behavior of area law with logarithmic corner corrections, and the obtained correction exponent represents the current central charge of the critical theory. Then we move on to the deconfined quantum critical point, where we still observe similar scaling behavior, but with a very different exponent. Namely, the corner correction exponent is found to be negative. Such a negative exponent is in sharp contrast with the positivity condition of the Rényi entanglement entropy, which holds for unitary conformal field theories (CFTs). Our results unambiguously reveal fundamental differences between DQC and quantum critical points described by unitary CFTs.

DOI: 10.1103/PhysRevLett.128.010601

Introduction.—Quantum many-body entanglement has become a fundamental organizing principle for the study of quantum matter. Scaling behavior of entanglement entropy (EE) provides deep insights into the structure of quantum many-body states and gives universal invariants that can be used to characterize distinct phases and phase transitions. For these reasons, EE has been of interest to many, ranging from the field theoretical to numerical and experimental communities of quantum many-body systems [1–20]. For $(2+1)$D quantum critical points, the EE obeys the "area law," i.e., linearly proportional to the perimeter of the entangling region. However, the subleading term turns out to be more interesting [1–5,20–24]: it is either a universal constant when the entangling region has a smooth boundary or a logarithmic term with a universal coefficient when the boundary contains sharp corners. The corner correction has been shown to be deeply related to intrinsic data of the underlying conformal field theory (CFT). For example, the universal coefficient for the von Neumann EE in the smooth limit is essentially given by the stress tensor central charge of the CFT. On the other hand, the scaling form of EE has also been investigated in numerical simulations of microscopic lattice models. In particular, the corner corrections were also identified in quantum Monte Carlo (QMC) simulations of quantum critical points (QCPs) for conventional symmetry-breaking transitions [14,15,17–19,25], the results of which are largely consistent with field-theoretical predictions.

For QCPs beyond the paradigm of Landau-Ginzburg-Wilson, the scaling forms of EE are not well understood. Among these, the quantum entanglement of the deconfined quantum criticality (DQC) [26–31]—a continuous quantum phase transition between two seemingly unrelated symmetry-breaking states—has not been explored much. Theoretically, since the proposed low-energy theory of DQC is a strongly coupled gauge theory [11,27,32,33], no controlled analytical treatment is available. While conventional O(n) CFTs are also interacting, they turn out to be

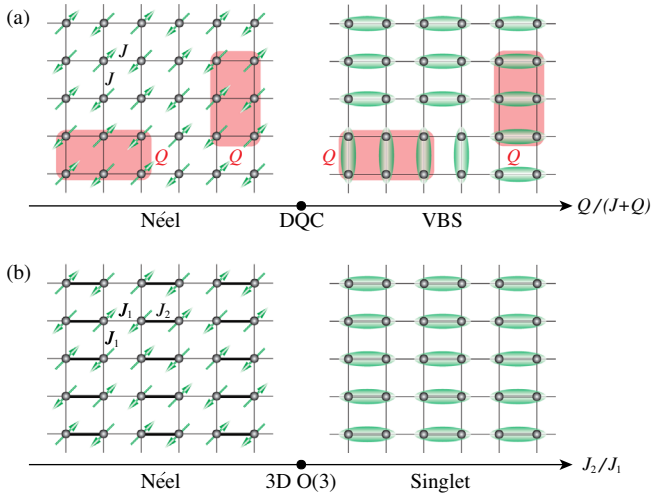

FIG. 1. The two lattice models: (a) the J-Q_3 model, which hosts DQC [52], (b) the square lattice J_1-J_2 antiferromagnetic columnar dimer model, which exhibits $(2+1)d$ O(3) QCP as J_2/J_1 is tuned [54].

"close" to the free Gaussian theory; e.g., the corner correction is well estimated by the value of the free theory. For DQC, a basic question such as whether the generic scaling form from CFT still holds is not known. In this Letter, we will address this question using large-scale, unbiased QMC simulations.

Because EE is a nonlocal quantity, its numerical computation, even just the second Rényi EE, is a challenging task in QMC simulations of interacting lattice models. Although several numerical algorithms have been developed for this purpose [6,12,13,16], they are still numerically very costly due to the necessity of enlarging the configurational space to replicas and exchanging them during the sampling processes. Further improving the efficiency and stability of the numerical estimator, especially for large system sizes and lattice models with multispin interactions or fermions [34,35], is still highly desirable.

These are the difficulties we set out to overcome in this Letter. Building on the recent nonequilibrium measurement of the Rényi entropy [36], which has shown its unprecedented efficiency on the measurement of Rényi entanglement entropy of the two-dimensional Heisenberg model than the previous attempts [37–41], we develop a new nonequilibrium increment method that can make the best usage of the divide-and-conquer procedure of the nonequilibrium process and the modern massive parallel computing technique to improve the speed of the simulation and the data quality of the entanglement measurement [42].

To test the performance of our method, we first show that at the $(2+1)$D O(3) transition in a square lattice J_1-J_2 columnar dimer model, the EE indeed exhibits universal scaling behavior of area law plus logarithmic corner corrections, and the obtained correction exponent is closer to the prediction of Gaussian theory [43] consistent with previous numerical results [14,17,18]. Then we move on to the DQC and find that, although the EE still obeys a similar scaling behavior, the universal coefficient of the corner correction term is negative. Such a result is in sharp contradiction with the positivity conditions for the Rényi EE that hold for unitary conformal field theories [10,44,45]—and pointing toward alternative scenarios of DQC such as nonunitary CFT with complex fixed points annihilation [45–47], multicriticality [33,48], or precursors to a weakly first-order transition [30,49–51].

Model.—Our main goal is to investigate the second Rényi EE at the deconfined QCP (DQCP) of the J-Q_3 model [26–28], as illustrated in Fig. 1(a). The Hamiltonian reads

$$H_{J-Q_3} = -J\sum_{\langle ij\rangle} P_{i,j} - Q\sum_{\langle ijklmn\rangle} P_{ij}P_{kl}P_{mn}, \tag{1}$$

where $P_{ij} = \frac{1}{4} - \mathbf{S}_i \cdot \mathbf{S}_j$ is the two-spin singlet projector. The quantum critical point separating the antiferromagnetic Néel and valence bond solid (VBS) states is at $[Q/(J+Q)]_c = 0.59864(4)$ [45,52,53].

We also investigate the square lattice columnar dimer model, shown in Fig. 1(b). The Hamiltonian is given by

$$H_{J_1-J_2} = J_1\sum_{\langle ij\rangle} \mathbf{S}_i \cdot \mathbf{S}_j + J_2\sum_{\langle ij\rangle'} \mathbf{S}_i \cdot \mathbf{S}_j, \tag{2}$$

where $\langle ij\rangle$ denotes the thin J_1 bond, $\langle ij\rangle'$ denotes the thick J_2 bond, and the QCP $(J_2/J_1)_c = 1.90951(1)$ [54] is known to fall within the $(2+1)$D O(3) universality class. As explained in the Supplemental Material [55], because of the translation symmetry breaking due to the strong J_2 and weak J_1 bonds in Eq. (2), the entangling region A must be chosen so that its boundary avoids strong dimer bonds to correctly extract the scaling behavior of EE from finite-size data.

At a conformally invariant QCP, the nth Rényi EE of an entangling region A of linear size l is expected to take the following form:

$$S_A^{(n)}(l) = a_n l - s_n \ln l + b_n. \tag{3}$$

Here s_n is a universal constant of the underlying CFT, which only depends on open angles of the sharp corners of A: $s_n = \sum_j s_n(\alpha_j)$, where α_j is the open angle [1,2,19]. Analytical results about the universal function $s_n(\alpha)$ are only available in the extreme cases $\alpha \to 0$ and $\alpha \to \pi$. In addition, one can prove that, generally, in a unitary CFT $s_n(\alpha)$ must be non-negative and is a concave function of α [3,10]. Numerically, the corner correction has been systematically investigated in $(2+1)$D O(n) models 19,25–14,15,17]]. Our goal is to extract s for the second Rényi entropy at DQC for $\alpha = \pi/2$, since we will only consider rectangle regions.

Nonequilibrium increment method for entanglement entropy.—Precise determination of the value of corner corrections, especially at QCPs, is by no means an easy task. Below, we first introduce an improved estimator based on the nonequilibrium increment method, which can substantially increase the precision and efficiency of the computation of Rényi EE in QMC simulations [42].

The nth Rényi EE $S_A^{(n)} = \ln[\mathrm{Tr}(\rho_A^n)]/(1-n)$ at finite temperature can be reexpressed by the ratio of two partition functions $S_A^{(n)} = [1/(1-n)]\ln(\mathcal{Z}_A^{(n)}/\mathcal{Z}_\emptyset^{(n)})$, stemming from its trace structure in the path integral [1]. Here A is the entangled region. In the configuration space of QMC simulation [56,57], as shown in Fig. 2, $\mathcal{Z}_A^{(2)}$ is a partition function of two replicas with entangling region A glued together and its complement $\bar{A}$ independent. $\mathcal{Z}_\emptyset^{(2)}$ can be viewed as a special case of $\mathcal{Z}_A^{(2)}$, where A is an empty set.

To evaluate $S_A^{(2)}$ on lattice models, various QMC estimators have been introduced [6,12,13,16,36]. While nearly all the algorithms suffer from computational

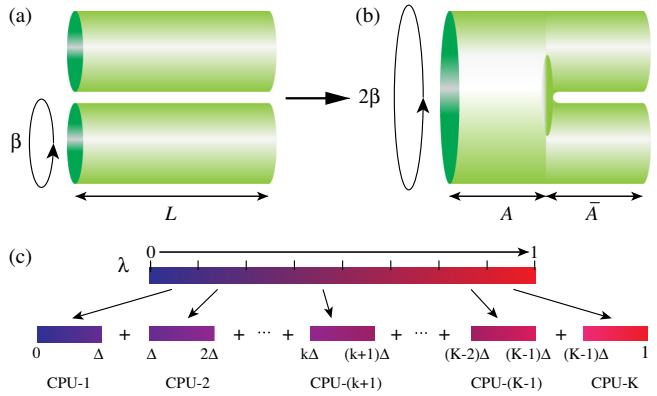

FIG. 2. The schematic diagram of the QMC configurations and the nonequilibrium increment method. (a) The QMC configuration of $\mathcal{Z}_{\varnothing}^{(2)}$. The configuration is two independent replicas with periodical boundary conditions. (b) The QMC configuration of $\mathcal{Z}_{A}^{(2)}$. The configuration is two replicas with the sites in the entangling region A glued together and sites in $\bar{A}$ with periodical boundary conditions. (c) The nonequilibrium increment process. We divide a nonequilibrium process that is characterized by λ evolving from $\lambda = 0$ to $\lambda = 1$ into K pieces. Each piece is independent of another and evolves from $\lambda = k\Delta$ to $\lambda = (k+1)\Delta$ with $k = 0, 1, \ldots, K-1$ and $\Delta = 1/K$. The final entanglement entropy is the summation of K such independent nonequilibrium pieces.

complexity—simulating replicas of the space-time configuration and connecting them with different boundary conditions—rendering poor quality data at low temperatures and large system sizes, the recent nonequilibrium measurement of the Rényi entanglement entropy [36] stands out for its reliability.

However, this method still has limitations (detailed analysis will be presented elsewhere [42]). For large systems, if the quench is not slow enough, then not all sites in A will join in the glued geometry at the end of the quench, leading to failure of the measurement. Although increasing the quench time can safely resolve this problem, it is often costly, as the simulation time significantly increases with the quench time. Such limitations heavily affect the computation of EE on larger systems, especially the more complicated models beyond nearest-neighbor Heisenberg.

Here we put forward an improved version of the nonequilibrium measurement—the nonequilibrium increment method—which can reduce the limitation of the nonequilibrium measurement on large systems. A schematic flow of the method is shown in Fig. 2(c). It can be seen that our method divides a nonequilibrium process into many smaller paralleled processes, and these smaller processes can be computed independently and thus are ideal for highly parallel simulations. In this way, the nonequilibrium increment method decreases the simulation time, as well as improves the data quality. We give a brief outline of our method below and will explain it in detail elsewhere [42].

In the nonequilibrium method [36], one introduces a function $\mathcal{Z}_A^{(n)}(\lambda)$, which is the sum of a collection of partition functions $Z_B^{(n)}$ weighted by $g_A(\lambda, N_B) = \lambda^{N_B}(1-\lambda)^{N_A - N_B}$, where B is a subset of the entangled region A, N_A is the total number of sites in A, and N_B is the total number of sites in B; the Rényi EE can be expressed as an integral over $\lambda \in [0, 1]$, $\mathcal{Z}_A^{(n)}(\lambda) = \sum_{B \subseteq A} g_A(\lambda, N_B) Z_B^{(n)}$, where $\mathcal{Z}_A^{(n)}(1) = \mathcal{Z}_A^{(n)}$ and $\mathcal{Z}_A^{(n)}(0) = \mathcal{Z}_{\varnothing}^{(n)}$. Thus, the entropy can be rewritten as $S_A^{(n)} = [1/(1-n)] \int_0^1 d\lambda [\partial \ln \mathcal{Z}_A^{(n)}(\lambda)/\partial\lambda]$. Reference [36] puts forward a nonequilibrium work defined as $W_A^{(n)} = -(1/\beta) \int_{t_i}^{t_f} dt \frac{d\lambda}{dt} [\partial \ln g_A(\lambda(t), N_B(t))/\partial\lambda]$ with $\lambda(t_i) = 0$ and $\lambda(t_f) = 1$. According to the Jarzynski equality [58], it can be proven that the entropy can be estimated by the work

$$S_A^{(n)} = \frac{1}{1-n} \ln(\langle e^{-\beta W_A^{(n)}} \rangle), \tag{4}$$

even when the nonequilibrium process is at finite rate. Our optimized method divides the integrating region [0, 1] into many small regions, e.g., $[0, \Delta], \ldots, [k\Delta, (k+1)\Delta], \ldots, [1-\Delta, 1]$, as shown in Fig. 2(c); then the nonequilibrium process can be seen as the sum of many small and independent nonequilibrium processes that can be simulated simultaneously. In this way, by means of massive parallel computing, we can greatly improve the data quality and reduce the simulation time.

We start from the following formula: $[\mathcal{Z}_A^{(n)}(1)/\mathcal{Z}_A^{(n)}(0)] = \prod_{k=1}^{K} [\mathcal{Z}_A^{(n)}(k\Delta)/\mathcal{Z}_A^{(n)}[(k-1)\Delta]]$, where K is an integer and $\Delta = (1/K)$, and rewrite the Rényi entanglement entropy as $S_A^{(n)} = [1/(1-n)] \sum_{k=0,1,\ldots,K-1} \int_{k\Delta}^{(k+1)\Delta} d\lambda [\partial \ln \mathcal{Z}_A^{(n)}(\lambda)/\partial\lambda]$. The argument for calculating the integral holds regardless of the lower and upper limits of the integral. As a result, we can apply the same argument on each individual integral and correspondingly get

$$S_A^{(n)} = \frac{1}{1-n} \sum_{k=0,1,\ldots,K-1} \ln(\langle e^{-\beta W_{k,A}^{(n)}} \rangle), \tag{5}$$

where $W_{k,A}^{(n)}$ is the work for the small piece between $\lambda(t_i) = k\Delta$ and $\lambda(t_f) = (k+1)\Delta$ in the nonequilibrium process. The detailed implementation protocol of our method is presented in the Supplemental Material [55]. We find such divide-and-conquer protocol gives very robust results of the Rényi EE. And since now the nonequilibrium process is carried out in parallel in hundreds or thousands of short processes, the speedup with the same factor and the increase of the data quality are self-evident.

Results.—With the nonequilibrium increment method at hand, we apply it to measure the second Rényi EE for the $H_{J_1-J_2}$ and H_{J-Q_3} models and reveal the scaling behavior of $S_A^{(2)}(L)$ at their corresponding QCPs.

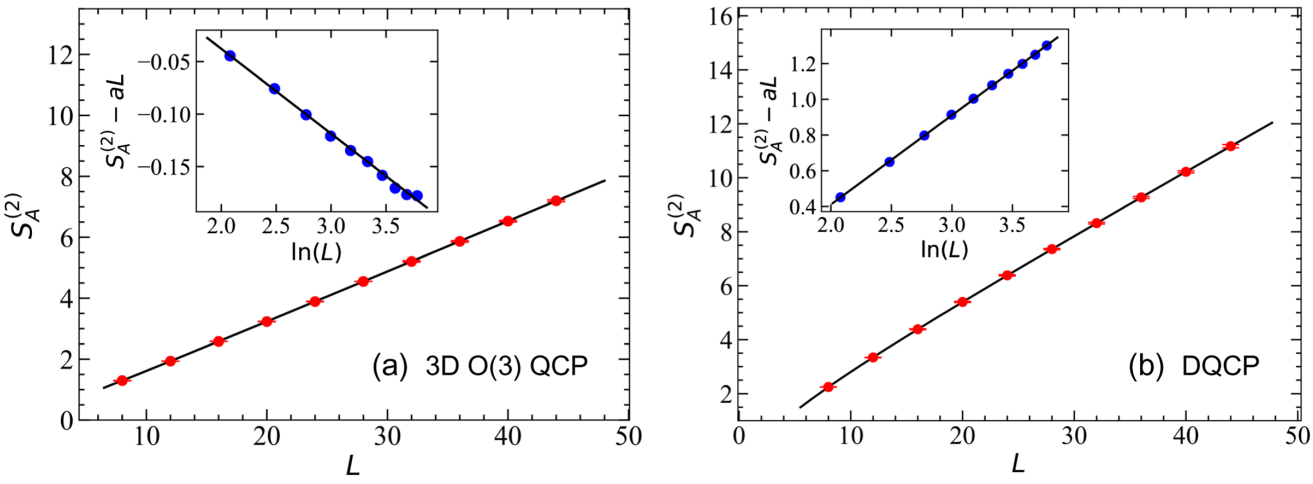

FIG. 3. $S_A^{(2)}(L)$ with even-B boundary of entangling region for (a) the $L \times L$ square lattice $H_{J_1-J_2}$ model at 3D O(3) QCP and (b) the H_{J-Q_3} model at DQCP with pinning field $\delta = 0.05$. The fitting result for $H_{J_1-J_2}$ is $S_A^{(2)}(L) = 0.168(1)L - 0.081(4)\ln(L) - 0.124(7)$. The fitting result for H_{J-Q_3} is $S_A^{(2)}(L) = 0.224(1)L + 0.49(1)\ln(L) - 0.58(2)$. Insets show the $S_A^{(2)} - aL$ versus $\ln(L)$ such that the sign of the log corrections manifest. It is clear that the DQC log correction acquires an opposite sign compared with the O(n) ones. This is in contrast to the positivity requirement of EE for unitary CFTs.

The main results are shown in Fig. 3. Since the columnar dimers in $H_{J_1-J_2}$ break the lattice translation symmetry, we test three different types of the entangling region A, denoted as odd, even A, and even B. Each type of region gives a different value of the area-law coefficient since they cut different kinds of bonds, which also strongly affects the estimate of the subleading corner correction. We find the even-B regions, whose boundaries do not cut any dimer and thus have the smallest area-law coefficient, yield the most robust finite-size scaling behavior. We therefore adopt such a geometry for both $H_{J_1-J_2}$ and H_{J-Q_3} presented here. Detailed discussions of the three different boundaries and their finite-size scaling behavior of $S_A^{(2)}(L)$ are presented in the Supplemental Material [55].

The main panel of Fig. 3(a) shows finite-size dependence of the $S_A^{(2)}(L)$ for the $H_{J_1-J_2}$ at its QCP. After fitting the data with Eq. (3), we obtain the coefficients a, s, and b. We find $s = 0.081(4)$, very close to the prediction of Gaussian theory. In the inset, we plot the EE after extracting the area-law contribution, i.e., $S_A^{(2)} - aL$ versus $\ln(L)$. The linear dependence is quite clear with a negative slope, i.e., $s > 0$.

We now turn to the DQC of H_{J-Q_3}. Here the model is manifestly translation invariant, so naively no special choice for the geometry of the entangling region is necessary. However, even at the DQC, the VBS domains still exist in a finite-size system and can still cause uncertainty in the EE. To reduce such finite-size error, we employ a small pinning field to lock the VBS order to a fixed configuration, which allows us to work consistently with the even-B regions [45,59]. The field is applied on the J_2 term such that $J_2 = J + (\delta/L)$; i.e., when extrapolating to the thermodynamic limit, the simulated Hamiltonian goes back to the original H_{J-Q_3}. We find the value of $\delta = 0.05$ gives the well-converged results of $S_A^{(2)}(L)$ and also note that, even without the pinning field $\delta = 0$, the same qualitative conclusion, as in Fig. 3(b), still holds (see the Supplemental Material [55] for details where such universal behavior of the negative log correction is persistently present from $\delta \in [0, 0.15]$, representing the robustness of our observation).

The fit of data in main panel of Fig. 3(b) according to Eq. (3) gives rise to $s = -0.49(1)$. After extracting the area-law contribution, as shown in the inset of $S_A^{(2)} - aL$ versus $\ln(L)$, a straight line with positive slope, i.e., $s < 0$, appears. Such large, negative value of s [one magnitude larger than that in the O(n) transition, the same large $s < 0$ also holds even when $\delta = 0$], is in sharp contrast to the expected corner corrections of the QCPs with CFT. It is from here that our results unambiguously reveal fundamental differences between DQC and QCPs described by unitary CFTs.

Discussion.—Our findings of the large and negative s in the second Rényi EE raise a number of intriguing questions about the theory of DQC. Since a negative s is not allowed in a unitary CFT, our observation appears to rule out such a description. This is consistent with a recent conformal bootstrap study, which finds tension between bounds following from unitary conformal invariance with the numerically computed critical exponents [32,60,61]. It is natural to connect these observations to the proposal that the observed regime of the DQC is controlled by a nonunitary fixed point very close to the physical parameter space [32,46,47,62], which implies approximate conformal invariance within a large length scale. However, it is not clear whether such a scenario can naturally explain a relatively large and negative s. Since the complex fixed point has to be very close to the physical parameter space,

one expects that the "nonunitarity," which manifests in, e.g., imaginary part of scaling dimensions, should be quite small. This is indeed the case in known examples of weakly first-order transition controlled by a complex CFT (note the suggestion that DQC is the precursor to a weakly first-order transition [30,49–51]), such as the $Q = 5$ Potts model in $(1 + 1)$D where the central charge, which is the coefficient of the log term in EE, appears to be a real positive number in numerical calculations [63]. Our results, however, suggest that the violation of unitarity is not just a small complex correction.

On the other hand, it is known that critical exponents of DQC exhibit unusual drift behavior with system size [60]. It is possible that similar drift also occurs for s, and, if this is the case, the formula (3) needs to be corrected. In fact, a generic feature of theories controlled by complex CFTs is that various universal quantities, such as scaling dimensions, exhibit drifting (or walking RG in technical terms) [64,65]. It is therefore important to more systematically understand the finite-size correction to s for complex CFTs, which we leave for future work. Other possible origins of the drift and how they affect the corner correction should also be investigated. For example, theoretically there exists a dangerously irrelevant operator at the critical point associated with the breaking of the emergent symmetry by lattice effect, which may introduce a new length scale in the problem. More recently, there is new evidence that shows the DQC is a multicritical point [48]; it will also be interesting to investigate the scaling of Rényi EE in such modified models to verify the theoretical [33] and numerical predictions [48] therein.

J. R. Z., Z. Y., and Z. Y. M. would like to thank Chenjie Wang for helpful discussions on the nonequilibrium process; they acknowledge support from the Research Grants Council of Hong Kong SAR of China (Grants No. 17303019, No. 17301420, and No. AoE/P-701/20), MOST through the National Key Research and Development Program (Grant No. 2016YFA0300502), and the Strategic Priority Research Program of the Chinese Academy of Sciences (Grant No. XDB33000000), the K. C. Wong Education Foundation (Grant No. GJTD-2020-01) and the Seed Funding Quantum-Inspired explainable-AI at the HKU-TCL Joint Research Centre for Artificial Intelligence. Y. C. W. acknowledges support from the NSFC under Grants No. 11804383 and No. 11975024, the NSF of Jiangsu Province under Grant No. BK20180637, and the Fundamental Research Funds for the Central Universities under Grant No. 2018QNA39. M. C. acknowledges support from NSF under Grant No. DMR-1846109 and the Alfred P. Sloan Foundation. We thank the Computational Initiative at the Faculty of Science and the Information Technology Services at the University of Hong Kong and the Tianhe platforms at the National Supercomputer Centers in Tianjin and Guangzhou for their technical support and generous allocation of CPU time. The authors acknowledge Beijing PARATERA Tech CO., Ltd. for providing high-performance computing resources that have contributed to the research results reported within this Letter.

*m.cheng@yale.edu
†zymeng@hku.hk

[1] P. Calabrese and J. Cardy, J. Stat. Mech. (2004) P06002.
[2] E. Fradkin and J. E. Moore, Phys. Rev. Lett. **97**, 050404 (2006).
[3] H. Casini and M. Huerta, Nucl. Phys. **B764**, 183 (2007).
[4] A. Kitaev and J. Preskill, Phys. Rev. Lett. **96**, 110404 (2006).
[5] M. Levin and X.-G. Wen, Phys. Rev. Lett. **96**, 110405 (2006).
[6] M. B. Hastings, I. González, A. B. Kallin, and R. G. Melko, Phys. Rev. Lett. **104**, 157201 (2010).
[7] M. A. Metlitski and T. Grover, arXiv:1112.5166.
[8] S. V. Isakov, M. B. Hastings, and R. G. Melko, Nat. Phys. **7**, 772 (2011).
[9] H.-C. Jiang, Z. Wang, and L. Balents, Nat. Phys. **8**, 902 (2012).
[10] H. Casini and M. Huerta, J. High Energy Phys. 11 (2012) 087.
[11] B. Swingle and T. Senthil, Phys. Rev. B **86**, 155131 (2012).
[12] S. Humeniuk and T. Roscilde, Phys. Rev. B **86**, 235116 (2012).
[13] S. Inglis and R. G. Melko, Phys. Rev. E **87**, 013306 (2013).
[14] S. Inglis and R. G. Melko, New J. Phys. **15**, 073048 (2013).
[15] A. B. Kallin, K. Hyatt, R. R. P. Singh, and R. G. Melko, Phys. Rev. Lett. **110**, 135702 (2013).
[16] D. J. Luitz, X. Plat, N. Laflorencie, and F. Alet, Phys. Rev. B **90**, 125105 (2014).
[17] A. B. Kallin, E. M. Stoudenmire, P. Fendley, R. R. P. Singh, and R. G. Melko, J. Stat. Mech. (2014) P06009.
[18] J. Helmes and S. Wessel, Phys. Rev. B **89**, 245120 (2014).
[19] N. Laflorencie, Phys. Rep. **646**, 1 (2016).
[20] M. M. Wolf, Phys. Rev. Lett. **96**, 010404 (2006).
[21] Y.-C. Lin, F. Iglói, and H. Rieger, Phys. Rev. Lett. **99**, 147202 (2007).
[22] R. Yu, H. Saleur, and S. Haas, Phys. Rev. B **77**, 140402(R) (2008).
[23] I. A. Kovács, F. Iglói, and J. Cardy, Phys. Rev. B **86**, 214203 (2012).
[24] I. A. Kovács and F. Iglói, Europhys. Lett. **97**, 67009 (2012).
[25] J. Zhao, Z. Yan, M. Cheng, and Z. Y. Meng, Phys. Rev. Research **3**, 033024 (2021).
[26] A. W. Sandvik, Phys. Rev. Lett. **98**, 227202 (2007).
[27] T. Senthil, L. Balents, S. Sachdev, A. Vishwanath, and M. P. A. Fisher, Phys. Rev. B **70**, 144407 (2004).
[28] N. Ma, G.-Y. Sun, Y.-Z. You, C. Xu, A. Vishwanath, A. W. Sandvik, and Z. Y. Meng, Phys. Rev. B **98**, 174421 (2018).
[29] Y. Liu, Z. Wang, T. Sato, M. Hohenadler, C. Wang, W. Guo, and F. F. Assaad, Nat. Commun. **10**, 2658 (2019).
[30] F.-J. Jiang, M. Nyfeler, S. Chandrasekharan, and U.-J. Wiese, J. Stat. Mech. (2008) P02009.
[31] D. Banerjee, F. J. Jiang, P. Widmer, and U. J. Wiese, J. Stat. Mech. (2013) P12010.

[32] C. Wang, A. Nahum, M. A. Metlitski, C. Xu, and T. Senthil, Phys. Rev. X **7**, 031051 (2017).
[33] D.-C. Lu, C. Xu, and Y.-Z. You, Phys. Rev. B **104**, 205142 (2021).
[34] T. Grover, Phys. Rev. Lett. **111**, 130402 (2013).
[35] F. F. Assaad, Phys. Rev. B **91**, 125146 (2015).
[36] J. D'Emidio, Phys. Rev. Lett. **124**, 110602 (2020).
[37] M. B. Hastings, I. González, A. B. Kallin, and R. G. Melko, Phys. Rev. Lett. **104**, 157201 (2010).
[38] H. F. Song, N. Laflorencie, S. Rachel, and K. Le Hur, Phys. Rev. B **83**, 224410 (2011).
[39] A. B. Kallin, M. B. Hastings, R. G. Melko, and R. R. P. Singh, Phys. Rev. B **84**, 165134 (2011).
[40] S. Humeniuk and T. Roscilde, Phys. Rev. B **86**, 235116 (2012).
[41] Z. Wang and E. J. Davis, Phys. Rev. A **102**, 062413 (2020).
[42] J. Zhao *et al.* (to be published).
[43] H. Casini and M. Huerta, Nucl. Phys. **B764**, 183 (2007).
[44] P. Bueno, R. C. Myers, and W. Witczak-Krempa, J. High Energy Phys. 09 (2015) 091.
[45] Y.-C. Wang, N. Ma, M. Cheng, and Z. Y. Meng, arXiv: 2106.01380.
[46] A. Nahum, Phys. Rev. B **102**, 201116(R) (2020).
[47] R. Ma and C. Wang, Phys. Rev. B **102**, 020407(R) (2020).
[48] B. Zhao, J. Takahashi, and A. W. Sandvik, Phys. Rev. Lett. **125**, 257204 (2020).
[49] A. B. Kuklov, M. Matsumoto, N. V. Prokof'ev, B. V. Svistunov, and M. Troyer, Phys. Rev. Lett. **101**, 050405 (2008).
[50] K. Chen, Y. Huang, Y. Deng, A. B. Kuklov, N. V. Prokof'ev, and B. V. Svistunov, Phys. Rev. Lett. **110**, 185701 (2013).
[51] J. D'Emidio, A. A. Eberharter, and A. M. Läuchli, arXiv: 2106.15462.
[52] J. Lou, A. W. Sandvik, and N. Kawashima, Phys. Rev. B **80**, 180414(R) (2009).
[53] J. Takahashi, B. Zhao, H. Shao, W. Guo, and A. W. Sandvik (unpublished). We thank Hui Shao for sharing unpublished data on the J-Q_3 model.
[54] N. Ma, P. Weinberg, H. Shao, W. Guo, D.-X. Yao, and A. W. Sandvik, Phys. Rev. Lett. **121**, 117202 (2018).
[55] See Supplemental Material at http://link.aps.org/supplemental/10.1103/PhysRevLett.128.010601 for the implementation protocol of the nonequilibrium increment of the Rényi entanglement entropy and details of the numerical results with the finite-size scaling with different boundary conditions of the entangling region.
[56] A. W. Sandvik, Phys. Rev. B **59**, R14157 (1999).
[57] O. F. Syljuåsen and A. W. Sandvik, Phys. Rev. E **66**, 046701 (2002).
[58] C. Jarzynski, Phys. Rev. Lett. **78**, 2690 (1997).
[59] F. F. Assaad and I. F. Herbut, Phys. Rev. X **3**, 031010 (2013).
[60] H. Shao, W. Guo, and A. W. Sandvik, Science **352**, 213 (2016).
[61] A. Nahum, J. T. Chalker, P. Serna, M. Ortuño, and A. M. Somoza, Phys. Rev. X **5**, 041048 (2015).
[62] Z. Wang, M. P. Zaletel, R. S. K. Mong, and F. F. Assaad, Phys. Rev. Lett. **126**, 045701 (2021).
[63] H. Ma and Y.-C. He, Phys. Rev. B **99**, 195130 (2019).
[64] V. Gorbenko, S. Rychkov, and B. Zan, J. High Energy Phys. 10 (2018) 108.
[65] V. Gorbenko, S. Rychkov, and B. Zan, SciPost Phys. **5**, 50 (2018).